

## Mechanistic Insight from Energy and Volume Profiles for CO Binding to a Lacunar Iron(II) Cyclidene Complex

Maria Buchalova,<sup>†,‡</sup> Daryle H. Busch,<sup>†</sup> and Rudi van Eldik<sup>\*‡</sup>

Department of Chemistry, University of Kansas, Lawrence, Kansas 66045, and Institute for Inorganic Chemistry, University of Erlangen-Nürnberg, Egerlandstrasse 1, 91058 Erlangen, Germany

Received September 5, 1997

### Introduction

There exists an ongoing interest in the chemistry of iron(II) dioxygen carriers, as is well documented by a number of reviews<sup>1–3</sup> reflecting the current state of knowledge and the development of the field. Many porphyrin-based model systems have been developed, and their properties and reactions have been summarized. Studies with dioxygen, the ligand of primary interest, are limited because of the destructive irreversible oxidation (autoxidation) reactions that accompany the ligand-binding process.

Iron(II) cyclidene<sup>4</sup> compounds (Figure 1) are non-porphyrin complexes that have received considerable attention as functional mimics for naturally occurring heme proteins. The binding reactions of small ligands, such as dioxygen and carbon monoxide, have been studied extensively.<sup>5,6</sup> A systematic investigation of the reactions of the series of iron(II) cyclidenes with carbon monoxide was performed<sup>7</sup> in order to elucidate the dependence of the kinetic and dynamic parameters on the structural features of these versatile compounds. Macrocyclic ligand substituents were found to have large effects on binding and dissociative rate constants, and steric interactions were found to dominate the observed effects.

We have devoted further attention to the mechanistic study of the reaction with carbon monoxide to attain a more detailed insight into the reactions of such small molecules with the iron(II) cyclidenes. Similar mechanistic studies have been successfully applied to the reactions of myoglobins and hemoglobins<sup>8–14</sup> with dioxygen and carbon monoxide, to some porphyrin-based

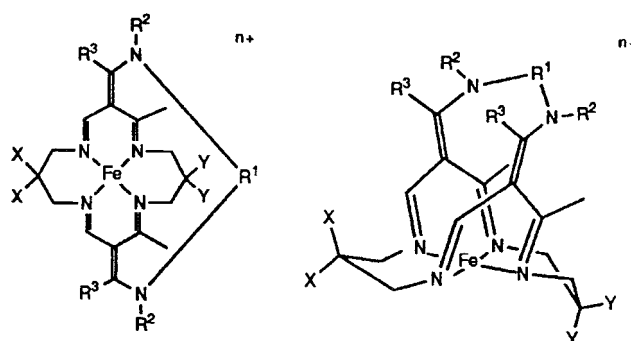


**Figure 1.** Planar and three-dimensional representations of the iron(II) cyclidene complexes  $[\text{Fe}^{\text{II}}(\text{PhBzXy})](\text{PF}_6)_2$ ,  $\text{R}^1 = m\text{-xylyl}$ ,  $\text{R}^2 = \text{benzyl}$ ,  $\text{R}^3 = \text{phenyl}$ .

model compounds,<sup>14</sup> and also to some cobalt(II) complexes<sup>15</sup> that bind dioxygen reversibly.

In this study, we investigated the temperature and pressure dependence of the association and dissociation of carbon monoxide to and from the iron(II) cyclidene complex  $[\text{Fe}^{\text{II}}(\text{PhBzXy})](\text{PF}_6)_2$  (Figure 1). From the reported thermodynamic parameters, the energy and volume profiles have been constructed and used as a basis for mechanistic interpretations and the elucidation of the nature of the transition state.

### Experimental Section

**Materials.** The iron(II) cyclidene complex  $[\text{Fe}(\text{PhBzXy})\text{Cl}]\text{PF}_6$  was prepared as described elsewhere.<sup>16</sup> The chloride counteranion was replaced by a simple metathesis procedure.<sup>17</sup> Acetonitrile, analytical grade, was dried over  $\text{P}_2\text{O}_5$  and subsequently distilled from  $\text{K}_2\text{CO}_3$ .<sup>18</sup> Tosylmethyl isocyanide (Aldrich) was used without further purification. Liquid reagents were degassed and transferred into the argon atmosphere glovebox. The carbon monoxide gas, 99.9% was obtained from Linde, AG. Nitrogen gas was purified by passing through an oxygen scavenger and molecular sieves in order to remove residual traces of oxygen and moisture, respectively.

The solutions for kinetic measurements were freshly prepared prior to measurements. The concentration of the complex solutions was within the range  $(1-5) \times 10^{-5}$  M. The solubility of carbon monoxide in acetonitrile used in our calculations was assumed<sup>7</sup> to be 6.6 mM at 25 °C and 1 atm. Solutions having carbon monoxide concentrations lower than saturation were prepared by mixing with  $\text{Ar}/\text{N}_2$ -saturated solutions, using Hamilton gastight syringes.

**Instrumentation.** Ambient-pressure stopped-flow experiments were performed using a Bio Sequential SX-18 MV stopped-flow reaction analyzer from Applied Photophysics Ltd. adapted for anaerobic conditions. The instrument allows temperature control within  $\pm 0.1$  °C. An observation optical path length of 10 mm was selected for our experiments.

High-pressure stopped-flow instrumentation described in the literature<sup>19</sup> was used to study the kinetics at elevated pressure. The complex solutions for the high-pressure measurements were prepared and filled into the syringes in the inert-atmosphere glovebox. The carbon

<sup>†</sup> University of Kansas.

<sup>‡</sup> University of Erlangen-Nürnberg.

- (1) Warburton, P. R.; Busch, D. H. Dynamics of Iron(II) and Cobalt(II) Dioxygen Carriers. In *Perspectives on Bioinorganic Chemistry*; Hay, R. W., Dilworth, J. R., Nolan, K. B., Eds.; JAI Press: London, 1993; Vol. 2, pp 1–79.
- (2) Momenteau, M.; Reed, C. A. *Chem. Rev.* **1994**, *94*, 659.
- (3) Feig, A. L.; Lippard, S. J. *Chem. Rev.* **1994**, *94*, 759.
- (4) Busch, D. H.; Alcock, N. W. *Chem. Rev.* **1994**, *94*, 585.
- (5) Busch, D. H.; Zimmer, L. L.; Grzybowski, J. J.; Olszanski, D. J.; Jackels, S. C.; Callahan, R. C.; Christoph, G. G. *Proc. Natl. Acad. Sci. U.S.A.* **1981**, *78*, 5919.
- (6) Herron, N.; Zimmer, L. L.; Grzybowski, J. J.; Olszanski, D. J.; Jackels, S. C.; Callahan, R. W.; Cameron, J. H.; Christoph, G. G.; Busch, D. H. *J. Am. Chem. Soc.* **1983**, *105*, 6585.
- (7) Buchalova, M.; Warburton, P. R.; van Eldik, R.; Busch, D. H. *J. Am. Chem. Soc.* **1997**, *119*, 5867.
- (8) Hasinoff, B. B. *Biochemistry* **1974**, *13*, 3111.
- (9) Adachi, S.; Morishima, I. *J. Biol. Chem.* **1989**, *264*, 18896.
- (10) Unno, M.; Ishimori, K.; Morishima, I. *Biochemistry* **1990**, *29*, 10199.
- (11) Unno, M.; Ishimori, K.; Morishima, I. *Biochemistry* **1991**, *30*, 10679.
- (12) Projahn, H.-D.; Dreher, C.; van Eldik, R. *J. Am. Chem. Soc.* **1990**, *112*, 17.

(13) Projahn, H.-D.; van Eldik, R. *Inorg. Chem.* **1991**, *30*, 3288.

(14) Taube, D. J.; Projahn, H.-D.; van Eldik, R.; Magde, D.; Traylor, T. G. *J. Am. Chem. Soc.* **1990**, *112*, 6880.

(15) Zhang, M.; van Eldik, R.; Espenson, J. H.; Bakac, A. *Inorg. Chem.* **1994**, *33*, 130.

(16) Cairns, C. J.; Busch, D. H. *Inorg. Synth.* **1990**, *27*, 261.

(17) Novotnak, G. C. Ph.D. Thesis, The Ohio State University, 1987.

(18) Perrin, D. D.; Armarego, W. L. F.; Perrin, D. R. *Purification of Laboratory Chemicals*, 2nd ed.; Pergamon Press: New York, 1980.

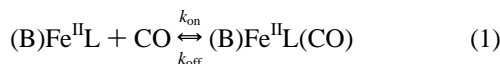
(19) van Eldik, R.; Gaede, W.; Wieland, S.; Kraft, J.; Spitzer, M.; Palmer, D. A. *Rev. Sci. Instrum.* **1993**, *64*, 1355.

monoxide solution was delivered to the high-pressure-cell assembly under ambient conditions. The temperature of the sample was controlled by the thermostated circulation system of the high-pressure cell. At elevated pressure, the solutions were kept for at least 20 min for temperature equilibration to  $25.0 \pm 0.1$  °C. Due to the relatively large scatter in the data, as is common for such air-sensitive compounds, sets of ca. 10 kinetic traces were recorded at least 4 times for every pressure. The resulting kinetic traces were evaluated using the KINFIT kinetic software package provided by On Line Instrument Systems (OLIS).

UV-vis spectra of samples at elevated pressures were measured on a Shimadzu UV 2100 spectrophotometer, equipped with a high-pressure cell, as described in the literature.<sup>20</sup> The high-pressure sample cell (pillbox cell) provides an optical path length of about 22 mm at ambient pressure. The temperature was controlled to  $\pm 0.1$  °C.

## Results

**Influence of Temperature and Pressure on the Kinetics of Reaction of Fe<sup>II</sup>L with CO.** The complex [Fe<sup>II</sup>(PhBzXy)](PF<sub>6</sub>)<sub>2</sub> exists in solution (acetonitrile) as a five-coordinate species.<sup>6</sup> Iron is surrounded by four nitrogen donors from the macrocycle in the equatorial positions. The outside axial position is presumably occupied by a coordinated solvent molecule (acetonitrile), whereas the second axial site is vacant and available for the binding of small ligands. The coordination of the sixth ligand to such iron(II) complexes can be followed by UV-vis spectral changes and is accompanied by a spin change on the metal center. The magnetic moment of the complex in acetonitrile solution has been determined<sup>6</sup> to be 4.99  $\mu_B$ , which indicates that solvent does not coordinate within the cavity and that the complex remains five-coordinate. It has been shown previously<sup>5</sup> that carbon monoxide binding to the five-coordinate, high-spin iron(II) center in cyclidene complexes, in the presence of a base molecule (B), can be described by the simple bimolecular process shown in eq 1. Coordination of



the sixth ligand, accompanied by a spin change at the iron(II) center, results in characteristic isosbestic spectral changes in the visible region of the spectra. Under pseudo-first-order conditions, the observed rate constant in the presence of excess CO is given by eq 2. For the complex under investigation,

$$k_{obs} = k_{off} + k_{on}[CO] \quad (2)$$

[Fe<sup>II</sup>(PhBzXy)(CH<sub>3</sub>CN)](PF<sub>6</sub>)<sub>2</sub>, the second-order binding rate constant,  $k_{on}$ , was determined at ambient conditions by the stopped-flow technique from the dependence of  $k_{obs}$  on the CO concentration. Our value of  $k_{on} = 9.9 \times 10^3 \text{ M}^{-1} \text{ s}^{-1}$  at 25 °C in acetonitrile, obtained from the slope of the linear plot (supplementary Figure S1 (Supporting Information)), is in close agreement with the previously determined value, using flash photolysis techniques,  $k_{on} = 6.4 \times 10^3 \text{ M}^{-1} \text{ s}^{-1}$ , under similar experimental conditions.<sup>7</sup>

The reaction of the iron(II) cyclidene with carbon monoxide was studied as a function of temperature in the range from 10 to 30 °C. The values of  $k_{on}$  determined from the CO concentration dependence of  $k_{obs}$  at five different temperatures are reported in the Eyring plot (Figure 2), and the activation enthalpy and activation entropy were estimated from the slope and the

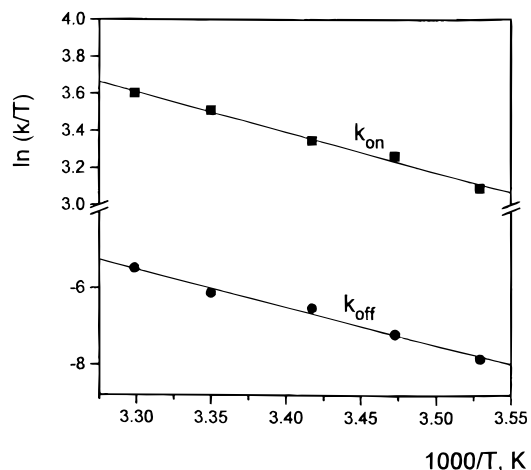


**Figure 2.** Eyring plot for the reaction of [Fe<sup>II</sup>(PhBzXy)](PF<sub>6</sub>)<sub>2</sub> with CO in acetonitrile at ambient pressure. Experimental conditions: for binding, [Fe<sup>II</sup>L] =  $3.2 \times 10^{-5}$  M,  $\lambda = 420$  nm; for dissociation, [Fe<sup>II</sup>L] =  $3.2 \times 10^{-5}$  M, [CO] =  $3.3 \times 10^{-3}$  M, [TMIC] =  $5 \times 10^{-2}$  M,  $\lambda = 370$  nm.

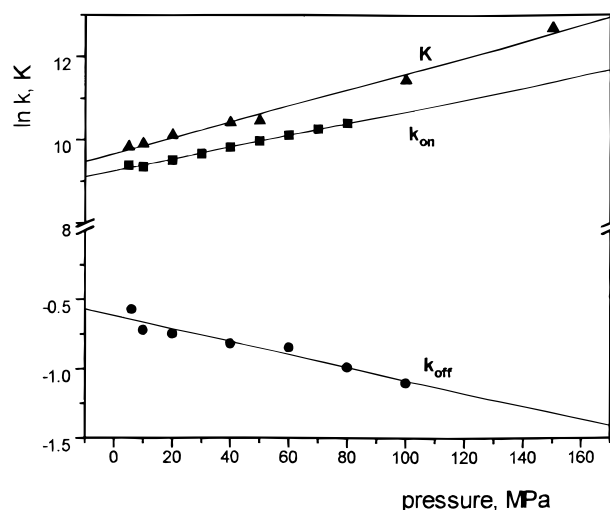


**Figure 3.** Pressure dependence of the equilibrium constant and association and dissociation rate constants for the reaction of [Fe<sup>II</sup>(PhBzXy)](PF<sub>6</sub>)<sub>2</sub> with CO in acetonitrile at 25 °C. Experimental conditions: for equilibrium studies, [Fe<sup>II</sup>L] =  $8.3 \times 10^{-5}$  M,  $\lambda = 420$  nm; for association process, [Fe<sup>II</sup>L] =  $2.3 \times 10^{-5}$  M, [CO] =  $3.3 \times 10^{-4}$  M,  $\lambda = 420$  nm; for dissociation process, [Fe<sup>II</sup>L] =  $5.0 \times 10^{-5}$  M, [CO] =  $8.3 \times 10^{-4}$  M, [TMIC] =  $5 \times 10^{-2}$  M,  $\lambda = 370$  nm.

intercept in the usual way. The corresponding values are  $\Delta H_{on}^{\ddagger} = 18 \pm 1 \text{ kJ mol}^{-1}$  and  $\Delta S_{on}^{\ddagger} = -108 \pm 4 \text{ J mol}^{-1} \text{ K}^{-1}$ .

The pressure dependence of the forward reaction for CO binding was studied by the stopped-flow technique in the range from 5 to 80 MPa. The reaction rate increases drastically with increasing pressure, and even for the lowest accessible carbon monoxide concentration chosen for our experiments, the kinetic measurements at pressures higher than 80 MPa were limited by the mixing time of the instrument. A CO concentration of 0.33 mM was selected to study the pressure dependence of the observed rate constant for the binding of CO. Under the employed experimental conditions, the reverse reaction is no longer negligible. The data from the pressure dependence of the reverse reaction (see below) were used to correct the observed rate constants for CO binding according to eq 2. The plot of the second-order binding rate constant ( $k_{on}$ ) versus pressure is linear, as shown in Figure 3. The value of the

(20) Fleischman, F. K.; Conze, E. G.; Stranks, D. R.; Kelm, H. *Rev. Sci. Instrum.* **1974**, *45*, 1427.

**Table 1.** Thermodynamic Parameters for the Reaction of the Fe(II) Cyclidene Complex and Myoglobin with CO

complex	parameter	Fe + CO → FeCO association	FeCO → Fe + CO dissociation	Fe + CO ⇌ FeCO overall reaction
Fe <sup>II</sup> (cyclidene)	$\Delta G$ , kJ mol <sup>-1</sup>	50.2 ± 1.7	74.0 ± 3.8	-23.8 ± 4.2
	$\Delta H$ , kJ mol <sup>-1</sup>	18.0 ± 1.3	82.8 ± 2.9	-64.8 ± 3.2
	$\Delta S$ , J mol <sup>-1</sup> K <sup>-1</sup>	-107.5 ± 3.8	29.7 ± 8.4	-137.2 ± 9.2
myoglobin	$\Delta G$ , kJ mol <sup>-1</sup>	41.0 ± 1.0 <sup>a</sup>	80.3 <sup>b</sup>	-39.3
	$\Delta H$ , kJ mol <sup>-1</sup>	17.1 ± 0.8 <sup>a</sup>	61.9 <sup>b</sup>	-44.8
	$\Delta S$ , J mol <sup>-1</sup> K <sup>-1</sup>	-81.2 ± 2.1 <sup>a</sup>	-61.1 <sup>b</sup>	-20.1

<sup>a</sup> Reference 8. <sup>b</sup> Reference 13.

activation volume  $\Delta V^\ddagger_{\text{on}} = -36.7 \pm 0.9 \text{ cm}^3 \text{ mol}^{-1}$  was obtained from the slope of the plot according to eq 3.

$$\Delta V^\ddagger = -RT \left( \frac{\partial \ln k}{\partial p} \right)_T \quad (3)$$

The reverse rate constant,  $k_{\text{off}}$ , was determined by the method described in the literature,<sup>21</sup> which involves the displacement of the bound CO by tosylmethyl isocyanide. The reaction was studied in the presence of an excess of tosylmethyl isocyanide, under which condition the release of the CO becomes the rate-determining step of the displacement reaction and  $k_{\text{obs}}$  corresponds directly to  $k_{\text{off}}$ . The reaction was found to be independent of the carbon monoxide (0.33–3.3 mM) and tosylmethyl isocyanide (5–50 mM) concentrations within the given ranges. The observed value of  $k_{\text{off}} = 0.56 \text{ s}^{-1}$  in acetonitrile at 25 °C and ambient pressure is in reasonable agreement with the value  $k_{\text{off}} = 1.2 \text{ s}^{-1}$  obtained previously by calculation from  $K = k_{\text{on}}/k_{\text{off}}$ .

The temperature and pressure dependencies of the decarbonylation rate constant were studied by the stopped-flow technique in the ranges from 10 to 30 °C and from 0.1 to 100 MPa, respectively. The observed temperature and pressure dependencies are plotted in the Figures 2 and 3, respectively. The plots are linear over the ranges studied and the values obtained were  $\Delta H^\ddagger_{\text{off}} = 83 \pm 3 \text{ kJ mol}^{-1}$ ,  $\Delta S^\ddagger_{\text{off}} = +30 \pm 8 \text{ J mol}^{-1} \text{ K}^{-1}$ , and  $\Delta V^\ddagger_{\text{off}} = +11.6 \pm 0.7 \text{ cm}^3 \text{ mol}^{-1}$ .

From the activation parameters of the forward and reverse reactions, the overall enthalpy and entropy changes were estimated, and the data are listed in Table 1. The determined thermodynamic and activation parameters enable us to construct the complete energy and volume profiles for the binding of carbon monoxide to iron(II) cyclidene complexes.

**Influence of Pressure on the Equilibrium of the Reaction of Fe<sup>II</sup>L with CO.** The overall reaction volume for reaction 1 was determined according to the method described in the literature.<sup>12</sup> An equilibrium mixture of the coordinately unsaturated and carbonylated species was subsequently exposed to increasing pressure from 0.1 to 150 MPa, and the shift in equilibrium toward the product was then detectable from the absorbance changes, as shown in supplementary Figure S2 (Supporting Information). The equilibrium constant at ambient pressure was calculated from the measured kinetic parameters,  $K = k_{\text{on}}/k_{\text{off}} = 1.84 \times 10^4 \text{ M}^{-1}$ .

The equilibrium constants at elevated pressure were estimated from the absorbance changes at 420 nm, using extinction coefficients of  $1.67 \times 10^4$  and  $1.29 \times 10^4 \text{ M}^{-1} \text{ cm}^{-1}$  for Fe<sup>II</sup>L and Fe<sup>II</sup>LCO, respectively. The plot of  $\log K$  as a function of pressure is shown in Figure 3. The reaction volume estimated from the slope of the linear dependence is  $\Delta V^\circ = -47.7 \pm 2.4 \text{ cm}^3 \text{ mol}^{-1}$ . This thermodynamically determined value of  $\Delta V^\circ$  is in excellent agreement with the  $\Delta V^\circ$  estimated from the

difference in the kinetically determined volumes of activation,  $\Delta V^\circ = \Delta V^\ddagger_{\text{on}} - \Delta V^\ddagger_{\text{off}} = -48.3 \pm 1.1 \text{ cm}^3 \text{ mol}^{-1}$ .

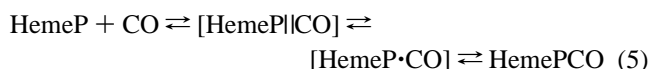
## Discussion

The binding of carbon monoxide to the iron(II) center in heme model complexes is usually described<sup>14</sup> in terms of a three-stage process (eq 4). In eq 4 the [Heme·CO] intermediate is a



geminate contact pair, in which the CO molecule is not coordinated to the iron, but it is present in a kinetically distinct position within the heme pocket.

In the process of CO binding to heme proteins (HemeP), a four-stage mechanism has been defined<sup>14</sup> according to eq 5. The



additional intermediate, [HemeP|CO], is the so-called protein-separated pair, in which CO is dispersed within the protein matrix. High-pressure kinetic studies on heme proteins and some model porphyrin compounds<sup>8–14</sup> established that the rate-determining step in eqs 4 and 5 is bond formation between the iron center and the CO molecule. Negative activation volumes for the overall CO association rate constant have been found for several heme proteins and model compounds;<sup>8,9,10,14</sup> see supplementary Table S1 (Supporting Information). The positive values of  $\Delta V^\ddagger_{\text{on}}$ , found for the reactions of dioxygen or other ligands with heme compounds,<sup>8,9,12</sup> were associated with ligand entry, or the diffusion process through the protein matrix, as the rate-limiting step. Moreover, the activation entropy often corresponds in sign to the activation volume; i.e., positive/negative activation volumes are accompanied by positive/negative activation entropies.<sup>22</sup>

In general, bond formation is expected<sup>23</sup> to show a negative value of  $\Delta V^\ddagger_{\text{on}}$ . The quantitative interpretation of  $\Delta V^\ddagger_{\text{on}}$  for reaction 4 can include several contributions, such as the intrinsic volume change (negative contribution) due to an overlap of van der Waals spheres during the bond-forming process, and contributions that arise from a spin change on the ferrous center, i.e., quintet to singlet transition (negative contribution), desolvation processes of the binding ligand (positive contribution), and in the case of the heme proteins also positive contributions associated with the structural changes in the protein matrix.

The energy, entropy, and volume profiles for carbon monoxide binding to the iron(II) center in [Fe<sup>II</sup>(PhBzXy)(CH<sub>3</sub>CN)]-(PF<sub>6</sub>)<sub>2</sub> are presented in Figures 4 and 5. The energy profile (Figure 4a) clearly shows that the activation barrier for the forward reaction is significantly smaller than that for the back-reaction, which results in a substantially negative reaction free enthalpy. Furthermore, the association process is characterized

(21) Traylor, T. G.; Tsuchiya, S.; Campbell, D. H.; Mitchell, M. J.; Stynes, D. V.; Koga, N. *J. Am. Chem. Soc.* **1985**, *107*, 604.

(22) van Eldik, R.; Asano, T.; le Noble, W. J. *Chem. Rev.* **1989**, *89*, 549.

(23) van Eldik, R.; Kelm, H. *Rev. Phys. Chem. Jpn.* **1980**, *50*, 185.

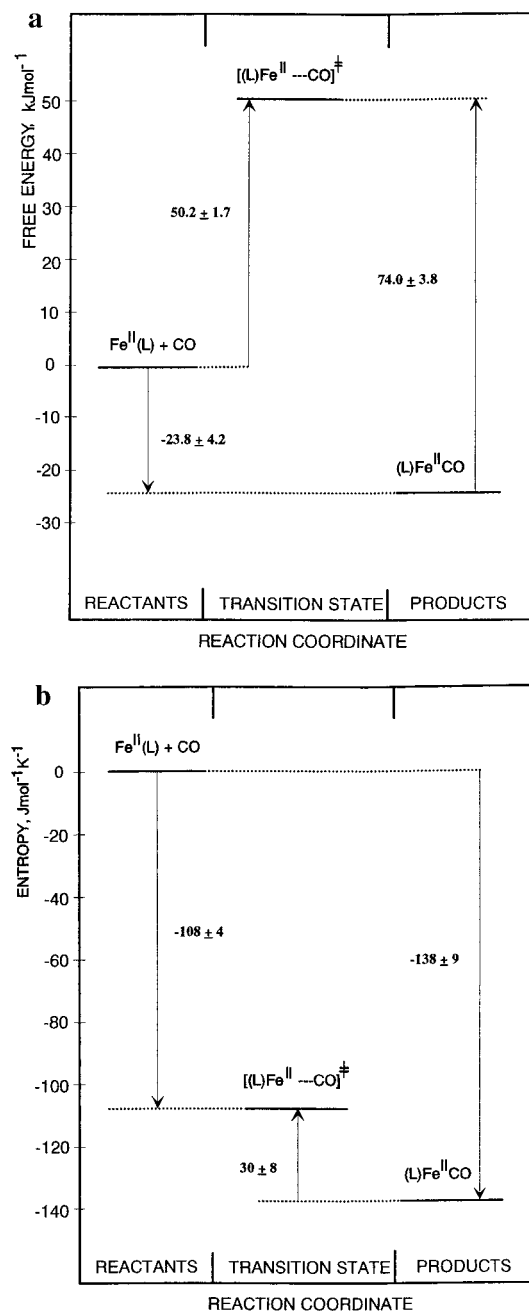


**Figure 4.** 4. Free energy (a) and entropy (b) diagrams for the reaction of  $[\text{Fe}^{\text{II}}(\text{PhBzXy})](\text{PF}_6)_2$  with CO in acetonitrile at 25 °C.

by a significantly negative activation entropy,  $\Delta S_{\text{on}}^{\ddagger} = -108 \text{ J mol}^{-1} \text{ K}^{-1}$  (Figure 4b), which is consistent with the entrance of CO into the cavity. Furthermore, the activation volume for the binding of CO is significantly negative,  $-36.7 \text{ cm}^3 \text{ mol}^{-1}$ . This volume collapse is very close to the partial molar volume of CO that has been reported in the literature to be  $33 \text{ cm}^3 \text{ mol}^{-1}$  in aqueous solution<sup>13</sup> and  $44 \text{ cm}^3 \text{ mol}^{-1}$  in 1,2-dichloroethane at 25 °C.<sup>24</sup> The apparent similarity of the values suggests that carbon monoxide completely disappears within the cavity of the complex in the transition state. Substantially positive contributions to  $\Delta S_{\text{on}}^{\ddagger}$  and  $\Delta V_{\text{on}}^{\ddagger}$  resulting from desolvation processes are not expected, since as it has been established previously<sup>6</sup> that the iron(II) cyclidenes exist in acetonitrile solution as five-coordinate species, with a vacant coordination site on the axial side protected by the ligand superstructure. In

(24) Schneider, K. J.; van Eldik, R. *Organometallics* **1990**, 9, 1235.

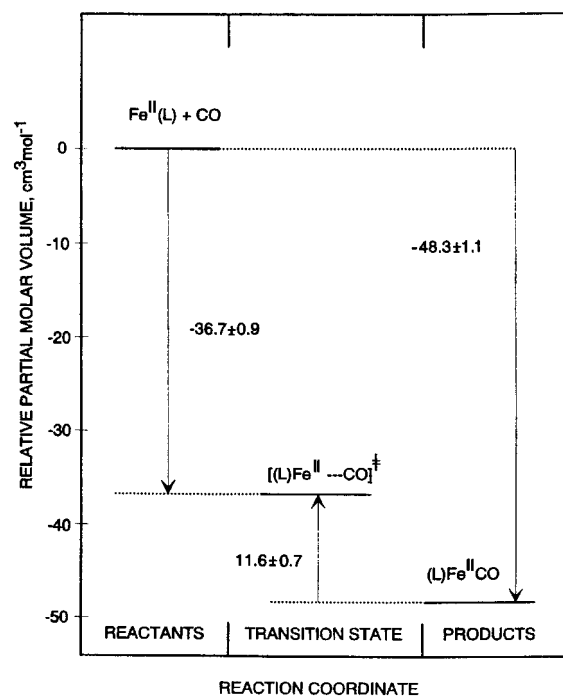


**Figure 5.** 5. Volume profile diagram for the reaction of  $[\text{Fe}^{\text{II}}(\text{PhBzXy})](\text{PF}_6)_2$  with CO in acetonitrile at 25 °C.

contrast, the dissociation of carbon monoxide, using tosylmethyl isocyanide, is characterized by a positive activation entropy,  $\Delta S_{\text{off}}^{\ddagger} = 30 \text{ J mol}^{-1} \text{ K}^{-1}$ , and a positive activation volume of  $+11.6 \text{ cm}^3 \text{ mol}^{-1}$ . In addition, the overall reaction volume is significantly more negative than that expected for only the disappearance of CO into the vacant site of the complex.

It is also known that Fe<sup>II</sup>–CO bond formation or bond breakage is accompanied by a spin change on the metal center. From structural studies on the five-coordinate, high-spin iron(II) cyclidene complexes,<sup>4</sup> it is known that the iron atom is displaced from the ligand plane. In forming the six-coordinate, low-spin iron(II) complex, the metal moves toward the plane of the equatorial nitrogens. Several studies have been reported on various iron(II) complexes that exist in high-spin–low-spin electronic state equilibria,<sup>25–28</sup> and those studies have shown that the volume changes associated with the spin transition of d<sup>6</sup> iron(II) fall in the range from 4 to 22  $\text{cm}^3 \text{ mol}^{-1}$ , depending on the solvent and ligand structure around the metal,<sup>25–27</sup> see supplementary Table S2 (Supporting Information). The volume of activation found for the dissociation of CO in the present study lies within this range of values and suggests that Fe–CO bond cleavage involves a LS to HS transition during which the metal center partially moves out of the ligand plane. In terms of the overall volume profile, this means that, during the binding of CO, the large volume collapse observed in going to the transition state is mainly associated with the disappearance of CO into the ligand pocket during partial Fe–CO bond formation. Following the transition state, there is a HS to LS change on the iron(II) center during which bond formation is completed and the metal center moves into the ligand plane. During the reverse process, the change in spin state accompanied by iron-

(25) DiBenedetto, J.; Arkle, V.; Goodwin, H. A.; Ford, P. C. *Inorg. Chem.* **1985**, 24, 456.

(26) McGarvey, J. J.; Lawthers, I.; Heremans, K.; Toftlund, H. *J. Chem. Soc., Chem. Commun.* **1984**, 1575.

(27) Beattie, J. K.; Binstead, R. A.; West, R. J. *J. Am. Chem. Soc.* **1978**, 100, 3044.

(28) Binstead, R. A.; Beattie, J. K.; Dewey, T. G.; Turner, D. H. *J. Am. Chem. Soc.* **1980**, 102, 6442.

(II) moving out of the ligand plane and partial Fe–CO bond cleavage is required in order to reach the transition state, after which CO escapes out of the ligand pocket and accounts for the large volume increase following the transition state. Thus the transition state for the process can be visualized as a high-spin iron(II)–CO species. The overall reaction volume of  $-47 \text{ cm}^3 \text{ mol}^{-1}$  therefore consists of ca.  $-35 \text{ cm}^3 \text{ mol}^{-1}$  for the binding of CO and ca.  $-12 \text{ cm}^3 \text{ mol}^{-1}$  for the HS to LS transition (see Figure 5).

This structural model comfortably accommodates both the volume and entropy profiles. The volume profile clearly demonstrates an early transition state in terms of Fe–CO bond formation for the forward reaction, corresponding prevalently to the volume change associated with entry of the CO into the cavity, and a late (product-like) transition state for the dissociation reaction, since the spin state has changed, implying substantial bond breakage and movement out of the ligand plane. The entropy changes reflect this same perspective on the extent of bonding. The iron is essentially unaltered at the transition state in the associative process. The large entropy change

corresponds mainly to the loss of the degrees of freedom of the CO. In the dissociative direction, the iron spin state has been changed from low spin to high spin and the bond has been greatly weakened, which is also indicated by a relatively large positive entropy change. The reverse reaction thus corresponds to a late transition state in terms of the Fe–CO bond breakage.

**Acknowledgment.** We gratefully acknowledge the DAAD, Deutsche Forschungsgemeinschaft, and Fonds der Chemische Industrie for financial support. We also thank Dr. Anton Neubrand for assistance with the high-pressure equipment.

**Supporting Information Available:** Tables S1 and S2, summarizing kinetic parameters for the reaction of several Fe(II) complexes with CO and thermodynamic parameters for the LS/HS equilibria of several Fe(II) complexes, and Figures S1 and S2, illustrating the determination of the second-order rate constant for the binding of CO and the determination of the reaction volume for the binding of CO (4 pages). Ordering information is given on any current masthead page.

IC9711426